

Microstructure and mechanical properties of chromium oxide coatings

Xiaolu Pang

Department of Materials Physics and Chemistry, University of Science and Technology Beijing, Beijing 100083, China; and Department of Mechanical Engineering, University of South Florida, Tampa, Florida 33620

Kewei Gao^{a)}

Department of Materials Physics and Chemistry, University of Science and Technology Beijing, Beijing 100083, China

Alex A. Volinsky

Department of Mechanical Engineering, University of South Florida, Tampa, Florida 33620

(Received 2 August 2007; accepted 12 September 2007)

Chromium oxide coatings were deposited on low-carbon steel by radiofrequency reactive magnetron sputtering at different oxygen flux values. X-ray diffraction, x-ray photoelectron spectroscopy, and high-resolution transmission electron microscopy were used to investigate the microstructure of chromium oxide coatings. Varying oxygen flux changed the coating microstructure; as with increasing oxygen flux the chromium oxide coating undergoes amorphous-to-crystalline transformation. The coating developed strong (300) texture at higher oxygen flux. Hardness, elastic modulus, wear resistance, and adhesion were investigated by nanoindentation and pin-on-disk tests. With changes in the coating microstructure as a function of increased oxygen flux, hardness, elastic modulus, and wear resistance were improved, but its adhesion was weakened.

I. INTRODUCTION

Chromium oxide is the hardest oxide that also exhibits low friction coefficient, high wear and corrosion resistance, and good optical and adiabatic characteristics. These properties allow for it to be used as a protective coating in tribological and microelectronic applications and as an adiabatic material in aeronautic and space fields.^{1–4} Many techniques have been developed to deposit chromium oxide coatings, including thermal plasma spraying, chemical vapor deposition, and ion implantation. Among them, reactive radiofrequency (rf) magnetron sputtering is most suitable for industrial production and makes it possible to achieve high-quality Cr₂O₃ stoichiometric coating with nearly 30 GPa hardness combined with good scratch resistance.⁵ The advantage of reactive magnetron sputtering for this purpose is mainly due to the high deposition rate achieved by sputtering from a metal target versus an oxide target.⁶

Mechanical and adhesion properties of coatings are affected by its microstructure. Sputtered coating microstructure and physical characteristics depend on the

deposition parameters,^{7–9} which in reactive sputter deposition play an important role to achieve a strictly stoichiometric ratio of Cr₂O₃; therefore, oxygen flux becomes especially important for oxidation. Different stoichiometric ratios exhibit vastly different mechanical properties in chromium oxide coatings.^{10–12}

High adhesion is known to ensure the prolonged lifetime of the coating and to promote good wear resistance.⁷ Good coating adhesion is required for wear- and corrosion-resistance applications. Premature failures can occur for many reasons, including coating delamination, cracking, and plastic deformation. In addition to this, thin ceramic physical vapor deposition (PVD) coatings usually have columnar grain structure with microcracks, pinholes, transient grain boundaries, and often high through-thickness porosity, which all lead to accelerated pitting corrosion and failure at the coating/substrate interface, especially in hostile environments.^{13–16} On the other hand, several studies show that coating thickness plays an important role in enhancing both PVD-coated cutting tool performance and resistance to abrasive and erosive wear,¹⁷ so it is important to understand the relationship between microstructure and mechanical properties of thick ceramic coatings.

In this paper x-ray diffraction (XRD), x-ray photoelectron spectroscopy (XPS), scanning electron microscopy (SEM), and transmission electron microscopy (TEM) techniques were used to characterize the microstructure

^{a)}Address all correspondence to this author.

e-mail: kwgao@mater.usf.edu.cn

DOI: 10.1557/JMR.2007.0445

of chromium oxide coating deposited with different oxygen partial pressure as a step toward developing a coating with good mechanical properties, namely, hardness, elastic modulus, wear resistance, and adhesion.

II. EXPERIMENTAL DETAILS

Chromium oxide coatings were deposited on low-carbon steel by a custom-built rf unbalanced reactive magnetron sputtering machine. The target used was high-purity 99.95% Cr. Depositions were performed at a total pressure of 10^{-1} Pa in a mixed Ar and O₂ atmosphere. The argon flow rate was 20 standard cubic centimeters per minute (sccm), target power was 350 W, while the oxygen flow rate ranged from 2.0 to 3.2 sccm with 0.3 sccm increments.

Before deposition, steel substrates were cleaned in acetone and ethanol for 10 min and consequently experienced 15 min in situ Ar plasma cleaning at rf power of 100 W to remove contaminants and to activate the substrate surface. A chromium interlayer was deposited on the substrates for 10 min, and then oxygen gas was introduced into the reaction chamber. The substrate temperature was around 473 K during a 1 h coating deposition.

The microstructure of chromium oxide coating was analyzed by XRD, XPS, and high-resolution TEM. The coating thickness was measured from SEM cross-section images. Hardness and reduced elastic modulus of the coatings were obtained by means of nanoindentation (Hysitron TriboIndenter, Minneapolis, MN) with a diamond Berkovich tip. Scratch tests were performed using Universal Micro-Tribometer-II (UMT) (Center for Tribology, Inc., Campbell, CA). The applied load on the conical (120° angle) diamond tip (200 μm radius) was continuously increased at a rate of 0.25 N/s, while the tip was moving at a constant velocity of 0.05 mm/s. An acoustic emission signal was used to monitor the coating and substrate damage.

Pin-on-disk wear tests were carried out with the UMT tribometer at room temperature in air. A Si₃N₄ ball was used as a coating wear counterpart. Normal load of 10 N was applied to the coating surface for 600 s. The circular wear track developed on the coating had a radius of 1.5 mm, and the ball linear sliding speed was 5 mm/s. In the ball-on-disk tests, the wear volume of the coating, V , was calculated by approximating the worn volume to a spherical cap. Assuming that the height of the cap is much smaller than the ball radius, the wear volume can be calculated as

$$V = 2\pi R \left[r^2 \sin^{-1} \left(\frac{w}{2r} \right) - \frac{w}{4} (4r^2 - w^2)^{1/2} \right], \quad (1)$$

where w is the wear scar width, measured by optical microscopy, R is the circular wear track radius, and r is the Si₃N₄ ball radius.¹⁸

III. RESULTS AND DISCUSSION

Figure 1 shows XRD patterns of chromium oxide coatings on low-carbon steel substrates. It can be seen from Figs. 1(a) and 1(b) that the oxygen flow rate of either 2.0 or 2.3 sccm (oxygen partial pressure of 6.6% and 7.5%, respectively) gives an amorphous coating. A few substrate diffraction peaks are present as well. Some crystalline Cr₂O₃ peaks appear in Fig. 1(c) when the oxygen flow rate was increased to 2.6 sccm, and a crystalline coating was obtained at 2.9 sccm, with no amorphous phase observed during TEM analysis of these specimens. It can be concluded that the chromium oxide coatings had completely transformed to the polycrystalline Cr₂O₃ phase at 2.9 sccm oxygen flux. At 3.2 sccm (10% oxygen partial pressure), the coating exhibited strong (300) texture. With increasing the number of oxygen ions, the probability of oxygen and chromium reaction increases, resulting in a larger amount of the crystalline Cr₂O₃ phase. Also, higher oxygen partial pressure increases the number of collisions between oxygen and chromium ions, so the coating is more apt to form a crystalline phase. The crystallization of the film can be affected by the atomic kinetic energy, which is determined by the oxygen partial pressure when other deposition parameters are fixed.¹⁵ Chromium oxide (300) preferred texture appears to be thermodynamically and kinetically favorable for the high oxygen partial pressure used in the deposition process.

XPS was used to infer the influence of the oxygen partial pressure on the chemical composition of the chromium oxide coating surface. Figures 2(a) and 2(b) show high-resolution Cr 2p XPS spectra of the chromium oxide coatings deposited with an oxygen flux of 2.3 and 3.2 sccm. All the binding energies were referenced to the C 1s peak centered at 284.6 eV. It can be seen from Fig.

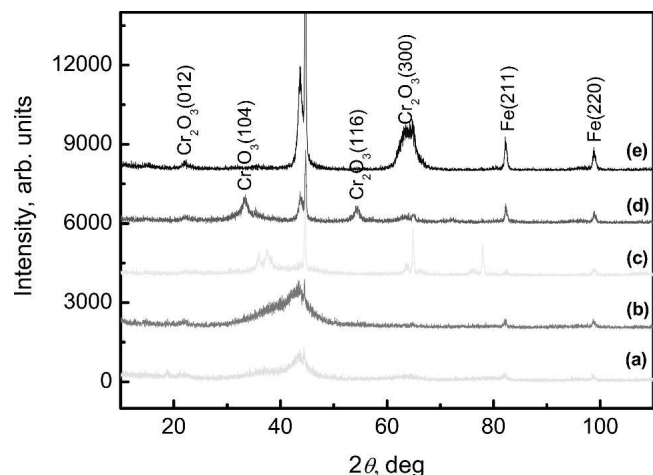


FIG. 1. XRD patterns of chromium oxide coatings deposited at different oxygen flux. (a) 2.0 sccm. (b) 2.3 sccm. (c) 2.6 sccm. (d) 2.9 sccm. (e) 3.2 sccm.

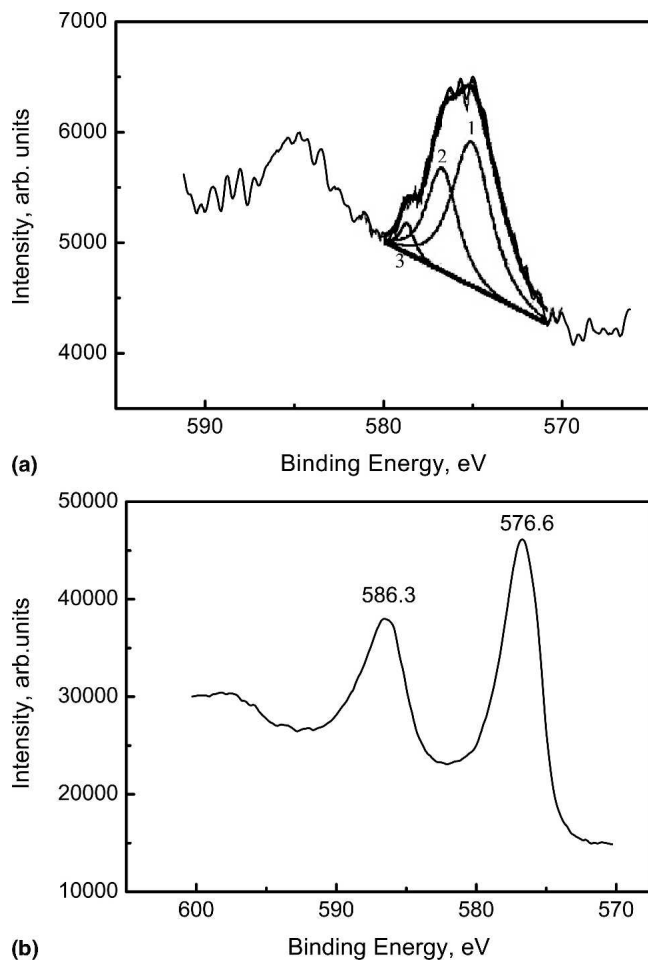
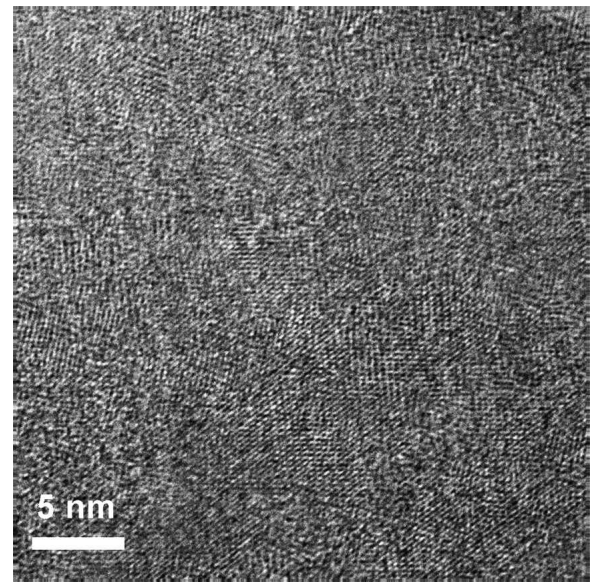


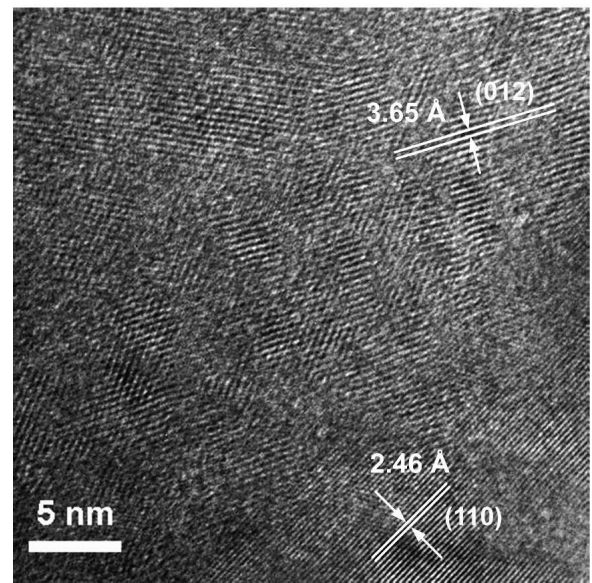
FIG. 2. XPS analysis of the chromium oxide coating surface. (a) 2.3 sccm and (b) 3.2 sccm.

2(a) that the Cr 2p spectrum can be curve fitted with three separate peak components at binding energies of 574.7, 576.6, and 578.3 eV, corresponding to metallic Cr, Cr_2O_3 , and CrO_3 , respectively.¹⁹ The intensity of each component was used to calculate its relative abundance on the chromium oxide coating surface. It is clearly observed that metallic Cr was the predominant species at the 2.3 sccm oxygen flux. The Cr 2p_{3/2} spectrum binding energy is 576.6 eV, which corresponds to Cr_2O_3 , the only species present at the 3.2 sccm oxygen flux, shown in Fig. 2(b). XPS can only detect elemental information from the top several nanometers of the sample surface, so the chemical composition deeper in the coating may be slightly different from these XPS results.

Figure 3 shows high-resolution TEM images of the chromium oxide coatings deposited at 2.6 and 3.2 sccm oxygen flux. In Fig. 3(a) coating material is predominantly amorphous, with some nanocrystalline grains surrounded by the amorphous phase, but the situation is much different in Fig. 3(b). The coating is almost totally crystalline in Fig. 3(b), which is also consistent with the



(a)



(b)

FIG. 3. HRTEM images of chromium oxide coatings deposited at (a) 2.6 sccm and (b) 3.2 sccm oxygen flux.

XRD results in Fig. 1. Precise measurements of the lattice spacing gives the interplanar distances of $d_1 = 0.365$ nm and $d_2 = 0.246$ nm, which could be referred to (012) and (110) Cr_2O_3 planes due to their similar d -spacing.²⁰ In theory, the distance of d_{012} is 0.363 nm and d_{110} is 0.248 nm for unstrained Cr_2O_3 . Residual stress in the coating can cause these parameters to change. The in-plane biaxial stress was calculated for the (300) textured films deposited at 3.2 sccm oxygen flux using:

$$\sigma = -\frac{E}{2\nu} \frac{d_{hkl} - d_0}{d_0}, \quad (2)$$

where σ is the biaxial stress in the film, E is the coating's elastic modulus, and ν is the Poisson's ratio of 0.25, d_{hkl} and d_0 are experimental and theoretical plane spacing values, respectively.²¹ The d_{300} of 0.1437 nm was calculated from the experimental XRD data in Fig. 1(e) using Bragg's law. The reduced modulus of 205 GPa at 3.2 sccm oxygen flux was measured by nanoindentation, and the elastic modulus of 234 GPa can be calculated from²²:

$$\frac{1}{E_r} = \frac{1 - \nu_{\text{sample}}^2}{E_{\text{sample}}} + \frac{1 - \nu_{\text{tip}}^2}{E_{\text{tip}}}, \quad (3)$$

where $E_{\text{tip}} = 1140$ GPa is the diamond elastic modulus, and $\nu_{\text{tip}} = 0.07$ is the diamond Poisson's ratio. Using Eq. (2) with $d_0 = 0.14314$ nm obtained from an unstrained sample,²⁰ one would calculate the in-plane biaxial compressive stress of about 2 GPa for the (300) textured chromium oxide coating. This seems to be consistent with the results obtained in TEM for similar isotropic films.²³

Figure 4 shows the hardness and elastic modulus of chromium oxide coatings obtained from nanoindentation tests performed to the depth below 10% of the coating thickness to avoid the substrate effects. There are no significant changes in either hardness or elastic modulus when the oxygen flux is below 2.6 sccm, but with the oxygen flux increasing above 2.6 sccm, the hardness and elastic modulus increase from 11–21 GPa and from 170–234 GPa, respectively. There is a significant change in the coating microstructure that occurs above 2.6 sccm oxygen flux, as it transforms from partially amorphous to fully crystalline coating (Figs. 1–3), so its hardness and elastic modulus increase.

Figure 5(a) shows SEM cross section of the chromium oxide coating including the Cr interlayer/substrate interface. The coating is quite dense with no pores or inclusions present. It survived mechanical polishing, so without any obvious stress concentrators in the coating or at

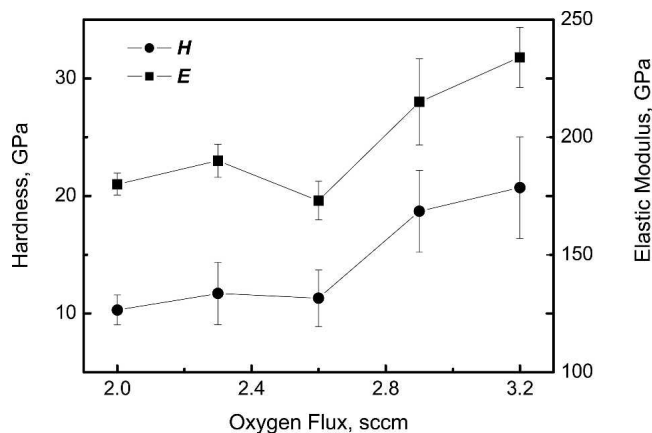


FIG. 4. Hardness and elastic modulus variations with oxygen flux.

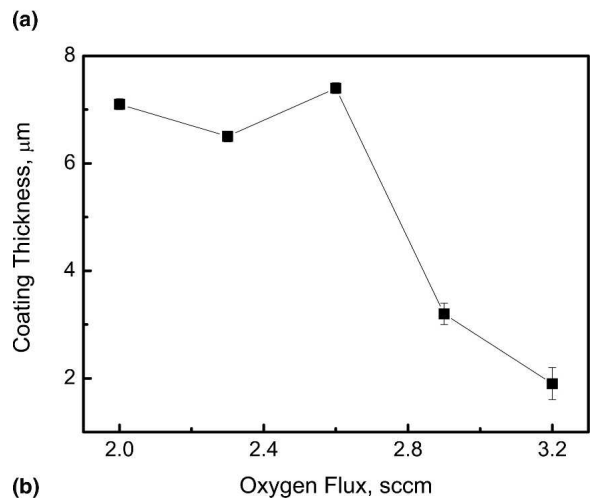
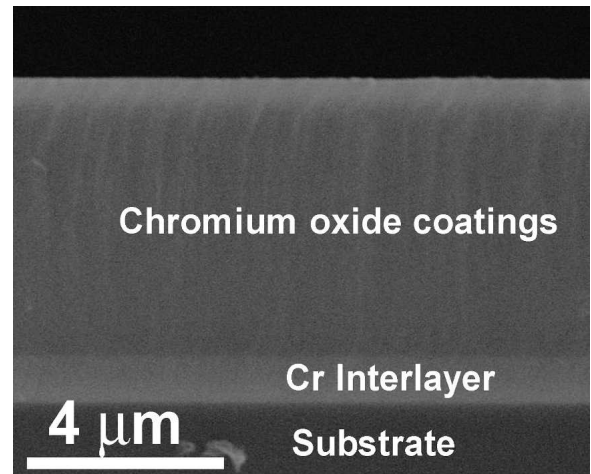


FIG. 5. (a) SEM image of the chromium oxide coating cross section and (b) coating thickness variations as a function of oxygen flux for the same deposition time.

the interface, one can expect good coating adhesion. Several studies show that a metal interlayer, 0.5 to 1.5 μm thick helps to accommodate coating residual stresses and allows for a thicker coating to be produced, with significant improvements in toughness, adhesion, and impact resistance.^{23–26} Figure 5(b) shows the chromium oxide coating thickness dependence on the oxygen flux values for the same deposition time, obtained from the SEM cross sections. The deposition rate at low oxygen flux is much higher than at high oxygen flux. The main reason is a higher number of oxygen ions with higher oxygen flux, which increases the ion collision probability.²⁷ Another reason is an oxide film forming on the chromium target surface, reducing the sputtering rate. The third is that if the target current remains constant with increased oxygen partial pressure, target poisoning effects take place.²⁸

A pin-on-disk machine was used to obtain the coatings friction by measuring the lateral force and wear resistance by assessing the change in the wear scar dimensions during sliding contact. Figure 6(a) shows the wear

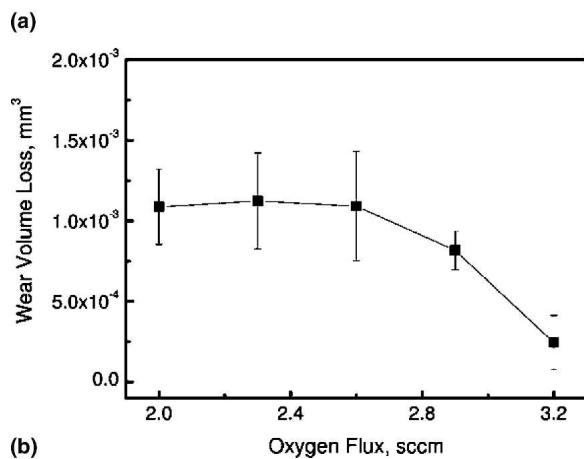
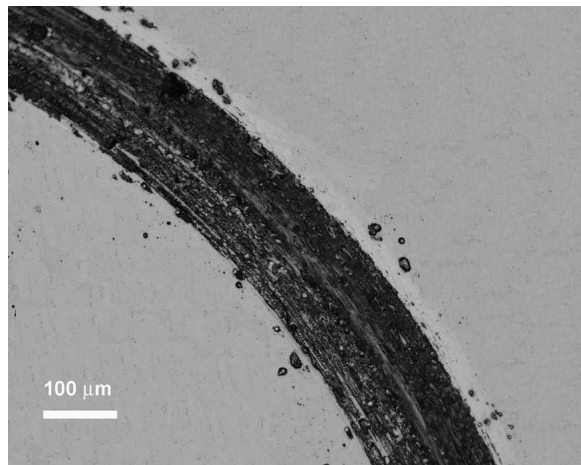


FIG. 6. (a) Wear track and (b) volume loss as a function of the oxygen flux.

scar of the chromium oxide coating; the width of the scar can be measured with optical microscopy, and the wear volume loss can be calculated using Eq. (1). Figure 6(b) shows the wear volume loss as a function of the oxygen flux. There are no significant changes in the wear volume loss when the oxygen flux is below 2.6 sccm, but the wear resistance is much higher for the high oxygen flux, since the wear resistance usually scales with hardness. At the same time, microstructure can influence wear resistance, and ceramic coating defects such as pinholes and microcracks also play an important role in wear. The wear resistance of chromium oxide can be improved by reducing the coating grain size and increasing its density.^{14,15}

Adhesion is one of the most important coating properties and can be assessed with the scratch test. The problem with this method is defining the critical lateral and normal forces. Figure 7(a) shows the lateral force and acoustic emission signal obtained during a scratch test. The critical lateral load is easily identified from the increased acoustic emission signal. The normal force was increased linearly during the scratch testing, so it was easily calculated at the point of coating delamination

obtained from the acoustic emission signal. Figure 7(b) shows the critical normal load of interfacial failures at different oxygen flux values. With increased oxygen flux, the critical normal load decreased, which may be caused by the coating intrinsic stresses. The in-plane biaxial compressive stress of chromium oxide coatings increases with oxygen partial pressure.³ The critical normal load also decreased because of the lower film thickness obtained at higher oxygen partial pressure.

Figure 7(c) gives the practical work of adhesion, which was calculated using Eq. (4), as a function of the oxygen flux. The minimum critical normal load, P_c at which delamination occurs is used to calculate the practical work of adhesion, W_A :

$$P_c = \frac{\pi r^2}{2} \left(\frac{2EW_A}{h} \right)^{1/2}, \quad (4)$$

where r is the contact radius determined from the width of the scratch track at the critical normal load [Figs. 7(d) and 7(e)] and h is the coating thickness.²⁹ The adhesion decreases from 195 to 62.5 J/m² with increasing oxygen flux. During sputter deposition oxygen ion energy increases with increased oxygen flux, which can cause a significant temperature rise, leading to higher residual stresses after cooling to room temperature. This effect deteriorated the adhesion strength of the coatings at higher oxygen flux.

The challenge lies in developing a method to produce these coatings with high hardness and wear resistance, while at the same time not sacrificing adhesion strength. This challenge can be solved by using the chromium metallic interlayer in the middle of the chromium oxide coating, which can be produced by intermittently turning off the oxygen flow during the reactive sputter deposition.^{23,26} A ductile chromium metal layer in the middle of the chromium oxide coating thickness also helps accommodate high residual stresses.

With relatively high adhesion above 50 J/m² one would also have to worry about the chromium oxide coating fracture toughness. We partially addressed this in terms of the wear resistance, although brittle coating fracture toughness can be measured by cube corner nanoindentation,³⁰ as well as other advanced techniques.^{31,32}

IV. CONCLUSIONS

The microstructure of chromium oxide coatings is alterable with different oxygen partial pressure in the rf magnetron reactive sputtering deposition technique. XRD, XPS, and TEM results show that the chromium oxide coatings were amorphous at low oxygen flux, but then transformed to textured polycrystalline at higher values of the oxygen flux. Reactive sputtering deposition

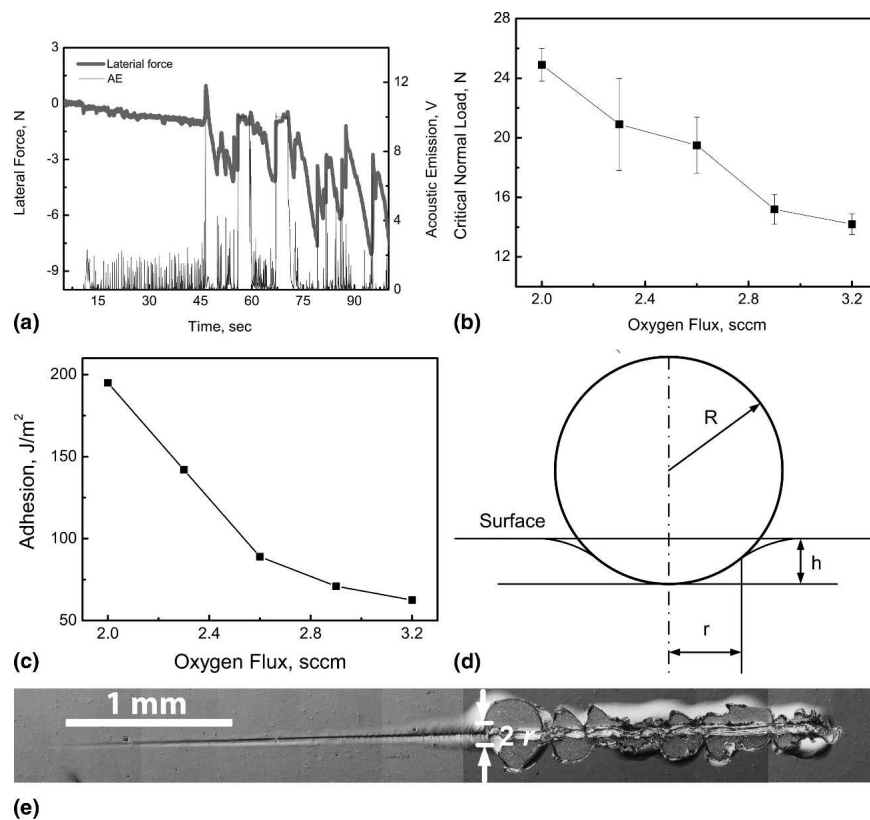


FIG. 7. (a) Critical lateral force determination for the coating failure during the scratch test. (b) Scratch test critical normal force as a function of the oxygen flux. (c) Adhesion of chromium oxide coatings at varying oxygen flux. (d) Schematic representation of scratch contact radius. (e) Scratch scar optical image.

rate decreases with increased oxygen flux. The hardness, elastic modulus, and wear resistance increased with higher values of oxygen flux, but the coating adhesion decreased.

ACKNOWLEDGMENTS

This work was supported by the National Natural Science Foundation of China (No. 50471091). Xiaolu Pang would like to acknowledge the support from the State Scholarship Fund of China (No. 20063037). Alex Volinsky would like to acknowledge the support from the National Science Foundation (CMMI-0600266, CMMI-0631526, and CMMI-0600231). We acknowledge help from Huisheng Yang, Yanbin Wang, and Lijie Qiao with sample preparation and mechanical testing.

REFERENCES

- F.D. Lai, C.Y. Huang, C.M. Chang, L.A. Wang, and W.C. Cheng: Ultra-thin Cr_2O_3 well-crystallized films for high transmittance APSM in ArF line. *Microelectron. Eng.* **67/68**, 17 (2003).
- E. Sourty, J.L. Sullivan, and M.D. Bijker: Chromium oxide coatings applied to magnetic tape heads for improved wear resistance. *Tribol. Int.* **36**, 389 (2003).
- P. Hones, M. Diserens, and F. Levy: Characterization of sputter-deposited chromium oxide thin films. *Surf. Coat. Technol.* **120/121**, 277 (1999).
- U. Rothhaar and H. Oechsner: Temperature induced dissolution of Cr_2O_3 into polycrystalline tantalum. *Thin Solid Films* **302**, 266 (1997).
- B. Bhushan, M.A.S.G. Theumissen, and X. Li: Tribological studies of chromium oxide films for magnetic recording applications. *Thin Solid Films* **311**, 67 (1997).
- P. Yashar, J. Rechner, M.S. Wong, W.D. Sproul, and S.A. Barnett: High-rate reactive sputtering of yttria-stabilized zirconia using pulsed d.c. power. *Surf. Coat. Technol.* **94/95**, 333 (1997).
- J.D. Olivas, C. Mireles, E. Acosta, and E.V. Barrera: Surface characterization of plasma spray metal deposition procedures using x-ray photoelectron spectroscopy. *Thin Solid Films* **299**, 143 (1997).
- I. Ozdemir, C. Tekmen, S.C. Okumus, and E. Celik: Thermal behaviour of plasma-sprayed Mo coating on cast-iron substrate. *Surf. Coat. Technol.* **174/175**, 1064 (2003).
- A. Forn, J.A. Picas, and M.J. Simon: Mechanical and tribological properties of Al-Si-Mo plasma-sprayed coatings. *J. Mater. Process. Technol.* **143/144**, 52 (2003).
- S.A. Kao, F.M. Doerner, and J.V. Novotny: Processing effects on the tribological characteristics of reactively sputtered chromium oxide (Cr_2O_3) overcoat films. *J. Appl. Phys.* **66**, 5315 (1989).
- G. Contoux, F. Cosset, A. Celerier, and J. Machet: Deposition process study of chromium oxide thin films obtained by d.c. magnetron sputtering. *Thin Solid Films* **292**, 75 (1997).
- B. Bhushan: Development of r.f. sputtered chromium oxide coating for wear application. *Thin Solid Films* **64**, 231 (1979).
- E. Andrade, M. Flores, S. Muhl, N.P. Barradas, G. Murillo,

- E.P. Zavala, and M.F. Rocha: Ion beam analysis of TiN/Ti multilayers deposited by magnetron sputtering. *Nucl. Instrum. Methods Phys. Res., Sect. B* **219/220**, 763 (2004).
14. J. Creus, H. Mazille, and H. Idrissi: Porosity evaluation of protective coatings onto steel, through electrochemical techniques. *Surf. Coat. Technol.* **130**, 224 (2000).
 15. C. Liu, A. Leyland, Q. Bi, and A. Matthews: Corrosion resistance of multi-layered plasma-assisted physical vapour deposition TiN and CrN coatings. *Surf. Coat. Technol.* **141**, 164 (2001).
 16. M. Fenker, M. Balzer, H.A. Jehn, H. Kappl, J.J. Lee, K-H. Lee, and H-S. Lee: Improvement of the corrosion resistance of hard wear resistant coatings by intermediate plasma etching or multi-layered structure. *Surf. Coat. Technol.* **150**, 101 (2002).
 17. K.D. Bouzakis, S. Hadjiyiannis, G. Skordaris, I. Mirisidis, N. Michailidis, and G. Erkens: Wear development on cemented carbide inserts, coated with variable film thickness in the cutting wedge region. *Surf. Coat. Technol.* **188/189**, 636 (2004).
 18. A.D. Sarkar: *Friction and Wear* (Academic Press, New York, 1940), p. 3.
 19. C.D. Wagner, W.M. Riggs, L.E. Davis, and J.F. Moulder: *Handbook of X-ray Photoelectron Spectroscopy*, (Perkin-Elmer, Pittsburgh, PA, 1979), p. 73.
 20. PDF Card No. 06-0694, PCPDFWIN, Version 2.02, JCPDS-ICDD, 1999.
 21. M. Murakami and R. Vook: Strain-relaxation mechanisms of thin deposited films. *Crit. Rev. Solid State Mater. Sci.* **11**, 317 (1983).
 22. K.L. Johnson: *Contact Mechanics* (Cambridge Press, Cambridge, UK, 1985), p. 153.
 23. X. Pang, K. Gao, H. Yang, L. Qiao, Y. Wang, and A.A. Volinsky: Interfacial microstructure of chromium oxide coatings. *Adv. Eng. Mater.* **9**, 594 (2007).
 24. A. Leyland and A. Matthews: Thick Ti/TiN multilayered coatings for abrasive and erosive wear resistance. *Surf. Coat. Technol.* **70**, 19 (1994).
 25. G.S. Kim, S.Y. Lee, J.H. Hahn, B.Y. Lee, J.G. Han, J.H. Lee, and S.Y. Lee: Effects of the thickness of Ti buffer layer on the mechanical properties of TiN coatings. *Surf. Coat. Technol.* **171**, 83 (2003).
 26. X. Pang, K. Gao, and A.A. Volinsky: Annealing effects on microstructure and mechanical properties of chromium oxide coatings. *Thin Solid Films* doi: 10.1016/j.tsf.2007.08.083 (2007).
 27. H. Choi, S. Choi, O. Anderson, and K. Bange: Influence of film density on residual stress and resistivity for Cu thin films deposited by bias sputtering. *Thin Solid Films* **358**, 202 (1999).
 28. G. Mohan Rao and S. Mohan: Studies on glow-discharge characteristics during dc reactive magnetron sputtering. *J. Appl. Phys.* **69**, 6652 (1991).
 29. A.A. Volinsky, N.R. Moody, and W.W. Gerberich: Interfacial toughness measurements for thin films on substrates. *Acta Mater.* **50**, 441 (2002).
 30. A.A. Volinsky, J.B. Vella, and W.W. Gerberich: Fracture toughness, adhesion and mechanical properties of low-K dielectric thin films measured by nanoindentation. *Thin Solid Films* **429**, 201 (2002).
 31. X.D. Li, D.F. Diao, and B. Bhushan: Fracture mechanisms of amorphous carbon films in nanoindentation. *Acta Mater.* **45**, 4453 (1997).
 32. B. Bhushan and X.D. Li: Nanomechanical characterization of solid surfaces and thin films. *Int. Mater. Rev.* **48**, 125 (2003).